The American Journal of Pathology, Vol. 182, No. 6, June 2013

ELSEVIER

The American Journal of PATHOLOGY

ajp.amjpathol.org

VASCULAR BIOLOGY, ATHEROSCLEROSIS, AND ENDOTHELIUM BIOLOGY

Endothelial GATA-6 Deficiency Promotes Pulmonary Arterial Hypertension

Angela Ghatnekar,* Izabela Chrobak,† Charlie Reese,* Lukasz Stawski,† Francesca Seta,‡ Elaine Wirrig,†§ Jesus Paez-Cortez,¶ Margaret Markiewicz,* Yoshihide Asano,*§ Russell Harley,‖ Richard Silver,* Carol Feghali-Bostwick,** and Maria Trojanowska*†

From the Division of Rheumatology and Immunology and the Departments of Regenerative Medicine and Cell Biology§ and Pathology,‖ Medical University of South Carolina, Charleston, South Carolina; the Arthritis Center,† the Whitaker Cardiovascular Institute,‡ and the Pulmonary Center,¶ Boston University, Boston, Massachusetts; and the Division of Pulmonary, Allergy, and Critical Care Medicine,** University of Pittsburgh, Pittsburgh, Pennsylvania*

Accepted for publication February 7, 2013.

Address correspondence to Maria Trojanowska, Ph.D., Boston University School of Medicine, 72 East Concord St., E-5, Boston, MA 02118. E-mail: trojanme@bu.edu.

Pulmonary arterial hypertension (PAH) is a chronic and progressive disease characterized by pulmonary vasculopathy with elevation of pulmonary artery pressure, often culminating in right ventricular failure. GATA-6, a member of the GATA family of zinc-finger transcription factors, is highly expressed in quiescent vasculature and is frequently lost during vascular injury. We hypothesized that endothelial GATA-6 may play a critical role in the molecular mechanisms underlying endothelial cell (EC) dysfunction in PAH. Here we report that GATA-6 is markedly reduced in pulmonary ECs lining both occluded and nonoccluded vessels in patients with idiopathic and systemic sclerosis-associated PAH. GATA-6 transcripts are also rapidly decreased in rodent PAH models. Endothelial GATA-6 is a direct transcriptional regulator of genes controlling vascular tone [endothelin-1, endothelin-1 receptor type A, and endothelial nitric oxide synthase (eNOS)], pro-inflammatory genes, CX3CL1 (fractalkine), 5-lipoxygenease-activating protein, and markers of vascular remodeling, including PAI-1 and RhoB. Mice with the genetic deletion of GATA-6 in ECs (Gata6-KO) spontaneously develop elevated pulmonary artery pressure and increased vessel muscularization, and these features are further exacerbated in response to hypoxia. Furthermore, innate immune cells including macrophages ($CD11b^+/F4/80^+$), granulocytes ($Ly6G^+/CD45^+$), and dendritic cells ($CD11b^+/CD11c^+$) are significantly increased in normoxic Gata6-KO mice. Together, our findings suggest a critical role of endothelial GATA-6 deficiency in development and disease progression in PAH. *(Am J Pathol 2013, 182: 2391–2406; http://dx.doi.org/10.1016/j.ajpath.2013.02.039)*

Pulmonary arterial hypertension (PAH) is a severe vascular disorder characterized by an increase in resistance and blood pressure in the pulmonary artery (PA) or lung vasculature.[1] The key pathological features of PAH occur in small PAs and include vasoconstriction, thrombosis, and inflammation, leading to intimal proliferation and fibrosis. Elevations in pulmonary vascular resistance and PA stiffness lead to pressure and volume overloading of the right ventricle, and eventually cause right heart failure and death. PAH is one of five groups within the pulmonary hypertension World Health Organization clinical classification system, which contains various forms including patients with idiopathic pulmonary arterial hypertension (IPAH) and familial pulmonary arterial hypertension (FPAH), and is associated with connective tissue diseases, primarily systemic sclerosis (SSc) pulmonary arterial hypertension (SSc-PAH).[1] SSc-PAH has similar clinical and histopathological features such as IPAH; however, it is unclear whether the molecular mechanisms responsible for the pathogenesis of the two forms are similar.[2]

The cellular and molecular processes underpinning pathological vascular remodeling in PAH are complex and involve phenotypic alterations in different cell types within the vascular wall with further contributions from the circulating immune and progenitor cells.[3] Although the inciting events remain poorly defined, current theories suggest that PAH is initiated by the disruption of EC homeostasis

Supported by NIH grants RO1 AR42334 (M.T.) and T32 AR 050958 (A.G.), and the Entelligence Young Investigators Award from Actelion Pharmaceuticals US, Inc. (A.G.).

Current address of E.W., The Heart Institute, Cincinnati Children's Hospital Medical Center, Cincinnati, OH; of Y.A., Department of Dermatology, University of Tokyo, Tokyo, Japan.

http://dx.doi.org/10.1016/j.ajpath.2013.02.039

leading to an imbalance of vasoactive factors and production of prothrombotic and pro-inflammatory mediators. Genetic studies have linked dysregulated bone morphogenetic protein signaling to the pathogenesis of FPAH and IPAH. Heterozygous mutations of the bone morphogenetic protein receptor type II (BMPR2) were found in 50% to 70% of FPAH cases and 11% to 40% sporadic of IPAH cases.[4] Furthermore, a subset of patients with hereditary hemorrhagic telangiectasia carrying mutations in activin receptor-like kinase or endoglin genes also develops PAH.[5] Consistently, mice with the genetic ablation of *Bmpr2* gene are predisposed to develop PAH.[6] In contrast to FPAH and IPAH, BMPR2 and activin receptor-like kinase 1 mutations, so far, were not found in patients with SSc-PAH, suggesting that other molecular mechanisms may underlie the disease process in SSc-PAH.[7,8] Notably, patients with SSc-PAH have higher disease mortality and are less responsive to currently used therapies compared to patients with IPAH.[9] In addition to autoimmunity, structural changes in systemic microcirculation and inflammation, present from an early stage of the disease, appear to be more severe in patients with SSc-PAH, and are likely to contribute to SSc-PAH.[9] Recent comprehensive gene analyses that compared lung tissues from patients with IPAH and SSc-PAH have further supported the role of inflammation in both forms of PAH.[10] The latter study has also revealed common and unique gene expression patterns in each disease. Despite recent advances in the elucidation of the cellular processes contributing to the development of PAH, the role of ECs in the initiation and progression of PAH remains poorly understood.

GATA-6 is one of six mammalian GATA factors that are highly conserved transcription factors with two tandem zinc fingers that interact with other transcriptional regulators and bind the canonical DNA motif, (G/A)GATA(A/T).[11] Human GATA-6 is expressed in a wide array of tissues (heart, lung, liver, kidney, pancreas, spleen, ovary, and small intestine), where it is believed to maintain the differentiated phenotype of the cells within these tissues.[12] GATA-6 is expressed in quiescent vascular smooth muscle cells (VSMCs) and may contribute to the maintenance of the contractile phenotype of VSMCs.[13,14] Furthermore, GATA-6 is rapidly decreased in proliferating VSMCs *in vitro*[12] and in injured vasculature.[15] Rescuing GATA-6 levels in a balloon-mediated injury of carotid arteries results in a higher degree of VSMC differentiation and significant reduction of neointimal formation in the rat.[15] Furthermore, GATA-6 functions as a transcriptional repressor of Tenascin C,[16] an extracellular matrix protein associated with progression of PAH.[17] These studies suggest that loss of GATA-6 may be a key component in the pathogenesis of injury-induced vascular lesions. GATA-6 is also significantly reduced in intramyocardial arteries of spontaneously hypertensive rats.[18] Importantly, GATA-6 transcript levels were found to be down-regulated concurrent with development and progression of pulmonary hypertension in rats.[19] Administration of simvastatin ameliorated increased pulmonary hypertension and vascular remodeling in this model, which correlated with normalization of GATA-6 expression levels.[19] Taken together, these observations indicate that GATA-6 may play a role in the phenotypic changes occurring during vascular remodeling in PAH.

Although GATA-6 vascular function has been investigated, mostly in VSMCs, a recent study has demonstrated that GATA-6 plays a vital role in angiogenesis and EC survival.[20] Importantly, compared transcriptomes of dermal microvascular ECs from normal subjects and patients affected by SSc revealed that GATA-6 may be down-regulated more than twofold in lesional skin with vasculopathy.[21] Given that GATA-6 is down-regulated in various animal models of vascular injury, the present study was undertaken to investigate the potential contribution of GATA-6 to the development of PAH focusing on the role of GATA-6 in ECs. We demonstrate that GATA-6 is down-regulated in pulmonary vascular lesions of PAH patients. Furthermore, the expression of GATA-6 is rapidly reduced in the monocrotaline (MCT) rat model and in the chronic hypoxia mouse model of PAH. Consistent with these findings, mice with the conditional knockdown of GATA-6 in ECs spontaneously develop elevated pulmonary arterial pressure and demonstrate increased vessel muscularization, as well as increased pulmonary inflammation. Microarray analysis coupled with chromatin immunoprecipitation assays reveal that GATA-6 regulates a set of genes linked to EC dysfunction previously associated with PAH. CX3CL1 (fractalkine) was among the genes that were significantly upregulated in GATA-6 deficient ECs, suggesting that GATA-6 down-regulation might also directly contribute to the increased inflammatory milieu. Together, these studies provide novel insights into the role of EC dysfunction during pathogenesis of PAH.

Materials and Methods

Immunohistochemical Analysis of Skin and Lung Specimens

The study group for the lung analysis included five IPAH lung specimens, nine SSc-PAH lung specimens, and four control specimens. Lung samples were obtained from patients with IPAH or SSc-PAH who underwent lung transplantation at the University of Pittsburgh Medical Center, under a protocol approved by institutional board review. Normal lung tissue specimens were obtained from donors, whose lungs were not used for tissue transplantation. Immunohistochemistry was performed on 4 μm serial sections using a Vectastain ABC kit (Vector Laboratories, Burlingame, CA) according to the manufacturer's instructions. Sections were subjected to a 5-minute antigen retrieval treatment in a stainless steel pressure cooker (Fagor, Basque Country, Spain) with antigen unmasking solution (Vector Laboratories, Burlingame, CA). Antibodies used included GATA-6 (1:100; Santa Cruz Biotechnology, Santa Cruz Biotechnology) or CD31 (1:1500; Santa Cruz Biotechnology). Binding of primary antibody to the tissue was visualized with 3.3′-diaminobenzidine solution

(Vector Laboratories, Burlingame, CA). Hematoxylin was used as a counterstain. Either normal rabbit or goat IgG was used as a control. The number of positively stained ECs in arterioles, venules, and capillaries were counted in more than 25 fields for each specimen. More than 120 vessels and 340 ECs were counted per specimen.

In Situ Hybridization

In situ hybridization was performed as described earlier.[22] Briefly, a 712-bp human GATA-6 probe was synthesized from a GATA-6 cDNA expression plasmid using the following primers: GATA-6 forward 5′-ATGACTCCAACTTCCACC-TCT-3′; GATA-6 reverse 5′-CAGCCTCCAGAGATGTGT-AC-3′. The PCR product was subject to digoxygenin-UTP labeling using the DIG (Sp6/T7) RNA labeling kit (Roche Diagnostics, Basel, Switzerland) and purification by RNeasy clean up kit (Qiagen, Hilden, Germany). Sections were incubated overnight with the GATA-6 sense or antisense probe (final concentration 200 ng/mL). Immuno-BCIP/NBT liquid substrate (MP Biomedicals, Santa Ana, CA) was used to detect hybridization. A poly d(T) probe was used as a control for intact RNA.

Cell Culture

Human PA ECs (HPAECs) were purchased from Lonza (Walkersville, MD) and cultured in complete endothelial growth medium-2. The cells were used at passage number 5−8 for all experiments.

Transfection of siRNA Oligos

Confluent cultures of HPAECs were transfected with 50 nmol/L of siRNA directed against GATA-6 (Dharmacon, Waltham, MA) and nonsilencing siRNA (Qiagen) using Genesilencer (Genlantis, San Diego, CA). Cells were incubated for 72 hours and either total RNA was prepared using TRI reagent (MRC, Inc., Cincinnati, OH) according to the manufacturer's protocol or whole cell extracts were prepared.

Quantitative RT-PCR

Quantitative RT-PCR was performed as previously described.[23] Sequences for all primers used in these studies are shown in Tables 1 and 2.

Immunoblotting for Cell Extracts

Nitrocellulose membranes were blocked with nonfat dry milk in T-TBS and then probed overnight with anti−GATA-6 (sc-9055; 1:500; Santa Cruz Biotechnology), anti-RhoB (sc-180; 1:250; Santa Cruz Biotechnology), anti−endothelial Nitric Oxide Synthase (eNOS; sc-654; 1:500; Santa Cruz Biotechnology), anti−MMP-1 (MAB3307; 1:1000; Millipore, Billerica MA), anti-MMP10 (MS-8220-PO; 1:500; NeoMarkers, Fremont, CA), or PAI-1 (395R; 1:250; American Diagnostics, Stamford, CT). Blots were incubated for at least 1 hour in the appropriate horseradish peroxidase coupled-secondary antibodies (1:3000) and developed using the Chemiluminescent detection kit (Pierce, Waltham, MA). Band intensities were determined by densitometric analysis.

ELISA

Cell culture supernatants were subjected to enzyme-linked immunosorbent assay (ELISA) using a human Quantikine CX3CL1 ELISA kit (R&D Systems, Minneapolis, MN) following the manufacturer's instructions.

Chromatin Immunoprecipitation

Chromatin immunoprecipitation was performed as previously described.[24] Relative fold enrichment of DNA was determined by PCR using specific primers for the indicated gene promoters (Table 3), followed by agarose gel electrophoresis. Primers that flank a region of genomic DNA between the glyceraldehydes-3-phosphate dehydrogenase gene and the CNAP1 gene were used a negative control.

Mice

Gata6flox/flox mice were purchased from Jackson Laboratory (Bar Harbor, ME). The mouse line, which contains *LoxP* elements in introns flanking exon 2 of the Gata-6 gene, was bred with mice expressing Cre recombinase under the control of the endothelial-specific VE-cadherin promoter (Jackson

Table 1 Primers Used for Human RT-qPCR

Gene	Primers	
PLA2G4C	5′-CCACTCACAACTTCCTGTACAAAC-3′	Forward
	5′-ATGGCTAAACCAGCATCCA-3′	Reverse
FLAP	5′-GTCTGCGGGGCTACTTTG-3′	Forward
	5′-TGCCTCACAAACAAGTACATCA-3′	Reverse
RhoB	5′-TAAGGGTGGTGATGGGTGAG-3′	Forward
	5′-GGGTTGGAAAGATGGTCAAG-3′	Reverse
MMP-10	5′-TGGACAGAAGATGCATCAGG-3′	Forward
	5′-CTTCAGTGTTGGCTGAGTGAA-3′	Reverse
MMP-1	5′-TCTGGGGTGTGGTGTCTCA-3′	Forward
	5′-GCCTCCCATCATTCTTCAGGTT-3′	Reverse
PAI-1	5′-CCCAGCTCATCAGCCACT-3′	Forward
	5′-GAGGTCGACTTCAGTCTCCAG-3′	Reverse
CX3CL1	5′-CCACCTTCTGCCATCTGAC-3′	Forward
	5′-ATGTTGCATTTCGTCACACC-3′	Reverse
eNOS	5′-AGGAACCTGTGTGACCCTCA-3′	Forward
	5′-TATCCAGGTCCATGCAGACA-3′	Reverse
ACE	5′-AACATGAGCAGGATCTACTCCAC-3′	Forward
	5′-AGCCAGGATGTTGGTGAGA-3′	Reverse
EDNRA	5′-CTCAACCTCTGCGCTCTTAGTG-3′	Forward
	5′-CCAAAGGAATCCCAATTCCC-3′	Reverse
ET-1	5′-GCTCGTCCCTGATGGATAAA-3′	Forward
	5′-CCATACGGAACAACGTGCT-3′	Reverse
GATA-6	5′-TTGTGGACTCTACATGAAACTCCA-3′	Forward
	5′-TTATGTTCTTAGGTTTTCGTTTCCTG-3′	Reverse

Table 2 Primers Used for Mouse RT-qPCR

Gene	Primers	
PLA2G4C	5′-GAGGACCTTCTGGCTGATTG-3′	Forward
	5′-CCAGCATGATGAGGAGTGAA-3′	Reverse
Flap	5′-CTGCTTCTCATCCCCTGATT-3′	Forward
	5′-TTGCGTTATGATGCGTCTCT-3′	Reverse
RhoB	5′-CAGACTGCCTGACATCTGCT-3′	Forward
	5′-GTGCCCACGCTAATTCTCAG-3′	Reverse
MMP-10	5′-AGGAAGTGACCCCACTCAC-3′	Forward
	5′-GGGTAAAAGTCTCCGTGTTCTC-3′	Reverse
Pai-1	5′-AGGATCGAGGTAAACGAGAGC-3′	Forward
	5′-GCGGGCTGAGATGACAAA-3′	Reverse
CX3CL1	5′-CGCGTTCTTCCATTTGTGTA-3′	Forward
	5′-CATGATTTCGCATTTCGTCA-3′	Reverse
eNOS	5′-CCAGTGCCCTGCTTCATC-3′	Forward
	5′-GCAGGGCAAGTTAGGATCAG-3′	Reverse
Ace	5′-TTGATGGAAGCATCACCAAG-3′	Forward
	5′-GGGCACAGACCCTGATACTT-3′	Reverse
EDNRA	5′-TGATCGTTTCATCTTCTTTCAATG-3′	Forward
	5′-CCTCATCAGACGGTCTTCCT-3′	Reverse
Et-1	5′-CTGCTGTTCGTGACTTTCCA-3′	Forward
	5′-TCTGCACTCCATTCTCAGCTC-3′	Reverse
Gata-6 (mouse)	5′-GGTGCTCCACAGCTTACAGG-3′	Forward
	5′-GCCGTCTCGTCTCCACAG-3′	Reverse
Gata-6 (rat)	5′-ACGCATGCGGTCTCTACAGT-3′	Forward
	5′-AGTCCAAGCCGTCGTGAT-3′	Reverse
Hif1a	5′-GCACTAGACAAAGTTCACCTGAGA-3′	Forward
	5′-CGCTATCCACATCAAAGCAA-3′	Reverse
Hif1b	5′-TGCCTCATCTGGTACTGCTG-3′	Forward
	5′-TGTCCTGTGGTCTGTCCAGT-3′	Reverse
Hif1a	5′-GGTTAAGGAACCCAGGTGCT-3′	Forward
	5′-GGGATTTCTCCTTCCTCAGC-3′	Reverse

Laboratory). For hypoxic conditions, mice were placed in a hypoxic chamber (10% oxygen) (BioSpherix, Lacona, NY).

Mouse EC Isolation

Two different methods were used to isolate mouse ECs. In the first method, lung and hearts were excised aseptically and transferred to ice-cold Dulbecco's modified Eagle's medium. Under the hood, the tissues were minced finely, followed by digestion in 15 mL of 1 mg/mL warm collagenase (Roche Diagnostics) at 37°C for 45 minutes with gentle agitation. The digested tissue was aspirated and transferred to a 20 mL syringe with a 14 g cannula attached and the clumps were triturated. The single cell suspension was then passed through a 70 μm cell strainer and subjected to centrifugation. The cell pellet was resuspended in 0.1% bovine serum albumin/PBS and anti-platelet EC adhesion molecule-1 antibody conjugated Dynabeads (Invitrogen, Carlsbad, CA) were added for 12 minutes with rotation. Beads were prepared according to the manufacturer's instructions. After washing, cells were plated on gelatin-coated 60 mm dishes. When cells were 70% to 80% confluent, they were sorted a second time with anti–ICAM-2 antibody-conjugated Dynabeads. Cultured ECs were characterized by a cobblestone morphology, uptake of fluorescent acetylated LDL (Biomedical Technologies Inc, Stoughton, MA), and specific staining for CD31. Cells were harvested at passages 2 to 3 for analyses.

In the second method, which was used for isolation of fresh cells for mRNA analyses, mouse lung tissue was finely minced and digested with 0.1 collagenase A (Roche Diagnostics), 2.4 units/mL dispase (Roche Diagnostics), and 6 units/mL DNase I (Qiagen) at 37°C for 1 hour. Debris was removed by sequential filtration through 70 and 40 μm filters (BD Biosciences, San Jose, CA). Cells were stained with fluorochrome-conjugated mouse-specific antibodies CD31-FITC/CD45-APC from BD Biosciences and then $CD31^{+}/CD45^{-}$ cells were sorted by MoFlo High Speed Cell Sorter (BD Biosciences).

Hemodynamic Analysis

Systolic blood pressure, diastolic blood pressure, mean pressure, heart pulse rate, and blood volume were measured noninvasively by determining the tail blood volume with a volume pressure recording sensor and an occlusion tail-cuff (CODA System; Kent Scientific, Torrington, CT).

Echocardiography

Transthoracic echocardiography was performed using a Vevo 770 High-Resolution Imaging System with 30-MHz RMV-707b scanning head (VisualSonics, Toronto, Canada). Pulmonary acceleration time (PAT) and PAT as a fraction of ejection time were measured from the pulse-wave Doppler recordings of the PA blood flow as previously described at baseline and after 1 month and 2 months of hypoxia.[25]

Table 3 Primers Used for ChIP

Promoter	Primers	
Negative control	5′-ATGGTTGCCACTGGGGATC-3′	Forward
	5′-TGCCAAAGCCTAGGGGAAGA-3′	Reverse
PLA2G4C	5′-ATGGCTCCACCAGGTAGGTA-3′	Forward
	5′-AGCTCATGAGGCTCTCCACA-3′	Reverse
FLAP	5′-CAGTGGTCCATGTTCCCTTT-3′	Forward
	5′-AGGTGGCTGCCTGGTATTCT-3′	Reverse
RhoB	5′-ACAGGCATGAGGTACTGTGC-3′	Forward
	5′-CGGTCTCTGTCAGTTGTTG-3′	Reverse
MMP-10	5′-TACCAAGCTTGTCAGCTCTG-3′	Forward
	5′-GGTGATACAGCCTACATCAG-3′	Reverse
MMP-1	5′-AATGCTGCCTAGCACCAAGG-3′	Forward
	5′-AGAGCCTTACCTGAGAAGAC-3′	Reverse
PAI-1	5′-AGGCAGGAGAACCACTTGAA-3′	Forward
	5′-ACTGGCTAGCAGTGGGTGAG-3′	Reverse
CX3CL1	5′-CTTCGGTGAGAGCCTGTTG-3′	Forward
	5′-CCCTGTTAGCCCAAAGAACA-3′	Reverse
eNOS	5′-TGGTGCCACATCACAGAAGG-3′	Forward
	5′-TCTAAAGCCTCAGCTCCACG-3′	Reverse
EDNRA	5′-CGCTGGAACCTTCCATAGTC-3′	Forward
	5′-AAGCTTAGAGGCCGTTGAGG-3′	Reverse
ET-1	5′-ATCTCCCCCTGGTGTTCTTC-3′	Forward
	5′-TTAGGCACATGCCCAGTCTT-3′	Reverse
VE-Cadherin	5′-GGTTCTTCTGGGCTCTGATC-3′	Forward
	5′-GGATATTGGGTGGAGTCAAG-3′	Reverse

ChIP, chromatin immunoprecipitation.

Measurement of RV Pressure

After the open chest method,[26] right ventricular (RV) pressures were measured using a high-fidelity pressure sensor catheter inserted directly into the right ventricle. Briefly, mice were anesthetized using isoflurane and mechanically ventilated through a 22-gauge cannula [130 breaths per minute, Harvard Apparatus (Holliston, MA) rodent ventilator]. Body temperatures were maintained on a heating pad. The thoracic cage was pulled upward by the xiphoid cartilage and the diaphragm was carefully removed to expose the heart. Cauterization of the tissue was used to minimize blood loss. The heart was superfused with a few drops of warm saline. The tip of a 25-guage needle was immersed in heparin solution (10,000 USP units/mL) and gently inserted into the right ventricle using the right coronary artery as a guide. The needle was retracted and the tip of a pressure catheter transducer (Micko-Tip, SPR-839; Millar Instruments, Houston, TX) was inserted through the small aperture. Pressure waveforms were recorded for at least 2 minutes for each mouse in real-time using the PowerLab Chart 5 version 5.3 data acquisition system and analysis software (ADInstruments, Colorado Springs, CO). RV pressures were calculated by averaging at least 20 cardiac cycles for each mouse.

Mouse Histology and Pulmonary Vascular Morphometry

Mice were euthanized by CO_2 gas and the right lung (with the heart) was inflated and fixed overnight in 4% paraformaldehyde. After fixation, the lung was dehydrated through a series of alcohol gradients and embedded in paraffin. Five μm sections were cut, deparaffinized in Histo-Clear (National Diagnostics, Atlanta, GA), and stained with an anti−α-smooth muscle actin antibody (dilution 1:800, clone 1A4; Sigma, St. Louis, MO), an anti−human von Willebrand factor antibody (dilution 1:800; Dako, Hamburg, Germany), and an anti−mouse Mac3 antibody (dilution 1:50; BD Pharminogen, San Jose, CA) using a Vectastain ABC kit (Vector Laboratories). Peripheral PAs ranging in 20 to 70 μm in size were counted in at least four fields at ×20 magnification with a Zeiss (Thornwood, NY) Axiovert-35 inverted microscope. Counted vessels were categorized into non-muscularized, partially muscularized (1% to 74% of medial layer has positive α-smooth muscle actin [SMA] staining), or fully muscularized (75% to 100% of medial layer has positive α-SMA staining). Percentages of vessels in each category were calculated by dividing the total number of vessels in each category by the total number of vessels counted in the field. Percent wall thickness (the thickness between the inner and outer boundary of the α-SMA-staining medial layer) was measured in fully muscularized PAs at two sites along the blood vessel using ImageJ software version 1.45s (NIH, Bethesda, MD). External diameters were measured concurrently for the same vessel and the percentage medial wall thickness was calculated as (wall thickness^1 + wall thickness^2) × 100 per external diameter.

Analysis of Cardiac Valves in Wt and Gata6 Conditional Knockout Mice

Hearts isolated from adult wild-type (Wt) and Gata6 conditional knockout mice were fixed in a 4% paraformaldehyde. Heart tissues were sectioned at 10 μm and stained with H&E, similar to previously described methods.[27] Valve histology was analyzed by comparison of serial sections of Wt (2) and Gata6-KO (3) mice under normoxic and hypoxic conditions.

Ventricular Weight Measurements

The ventricles were excised and weighed. The weight ratio of the right ventricle to the left ventricle plus septum was calculated as indices of RV hypertrophy.

MCT-Induced Rat Model of PAH

Male Sprague-Dawley rats (200 to 225 g body weight) were dosed with a single 60 mg/kg body mass subcutaneous injection of MCT. Control rats received an equal volume of saline. Rats were housed in a 12/12-light/dark cycle and given standard rat chow and water *ad libitum*. They were euthanized at 1, 3, 5, 10, and 20 days postinjection.

RNA Isolation from Mouse and Rat Lungs and Real Time-PCR

RNA was isolated and purified using the Qiagen RNeasy kit (Qiagen) following the manufacturer's instructions. RT-PCR was performed as previously described using the primers listed in Table 2.

Immunoprecipitation and Immunoblotting for Rat Lungs

Lungs were homogenized in radioimmunoprecipitation assay buffer using a douncer. Then 1000 μg of extract was pre-cleared with protein G-Sepharose beads (Amersham Biosciences, Pittsburgh, PA), and incubated with 1 μg of monoclonal mouse anti-GATA6 antibody (R&D Systems) overnight at 4°C with gentle rotation. Protein G-Sepharose beads were added and the precipitated proteins were subjected to SDS-PAGE. Immunoblotting for Gata-6 was performed as previously described for cell extracts. As an input control, 10 μL of the pre-cleared extract was subjected to SDS-PAGE and membranes were incubated with a mouse anti−β-actin antibody (1:5000, Sigma).

Rat Lung Histology and Immunohistochemistry

Sections (5 μm thick) were stained with Masson's trichrome stain and H&E stain using standard techniques. Immunohistochemical analysis was performed using the standard avidin-biotin-peroxidase method as previously described. Sections were incubated in primary antibody against α-SMA (Thermo Scientific, Neomarkers, Kalamazoo, MI).

Flow Cytometry Analysis

Flow cytometry was performed on an LSRII cytometer (BD Biosciences) and data were analyzed using FlowJo software version 6.3.2 (Tree Star Inc., Ashland, OR). Mouse lung tissue was finely minced and digested with 0.1 collagenase A (Roche Diagnostics), 2.4 units/mL dispase (Roche Diagnostics), and 6 units/mL DNase I (Qiagen) at 37°C for 1 hour. Debris was removed by sequential filtration through 70 and 40 μm filters (BD Bio-sciences). Cells were stained with fluorochrome-conjugated mouse-specific antibodies (T cells CD3-PE/CD45-APC, B cells B220-PE/CD45-APC, macrophages CD11b-FITC/F4/80-PE, granulocytes Ly6G-FITC/CD45-APC, and dendritic cells CD11b-FITC/CD11c-PerCP) from BD Biosciences.

Statistical Analysis

All data were analyzed by Student's paired *t*-test. Mouse data were also subjected to one-way analysis of variance with Bonferroni post hoc). The level for statistical significance was set at $P < 0.05$.

Results

GATA-6 Levels are Markedly Decreased in the Pulmonary Vasculature of SSc-PAH and IPAH Patients

We first examined expression of GATA-6 protein in lung specimens from nine patients with SSc-PAH, five patients with IPAH, and four healthy controls. Representative stainings are shown in Figure 1, A and B. In healthy controls, GATA-6 protein was detected in the nuclei of alveolar type II cells, VSMCs, and ECs; however, peripheral, slight, or no nuclear staining could be detected in ECs of SSc-PAH tissue and slight or no nuclear staining for GATA-6 could be seen in ECs of IPAH tissue. GATA-6 positive EC nuclei were counted in arterioles and venules for each lung specimen (Figure 1, A and B, respectively). The analysis revealed a significant reduction of GATA-6 in both vessel types, including occluded and nonoccluded, in both SSc-PAH and IPAH patients. Reduced expression of GATA-6 was also observed in the capillaries of PAH patients. In addition, GATA-6 protein levels were drastically decreased in VSMCs, but there were no apparent changes in the expression of GATA-6 in alveolar type II cells. To further analyze if GATA-6 is decreased at the mRNA level, we performed *in situ* hybridization studies (Figure 1C). The results demonstrated that GATA-6 is abundantly expressed in ECs lining arterioles and venules in normal controls, but is strikingly decreased in ECs lining both vessel types in IPAH patients. These observations suggest that GATA-6 deficiency may contribute to vessel remodeling during PAH.

GATA-6 Regulates Expression of Genes Involved in Vascular Remodeling

In an effort to begin to understand how loss of GATA-6 in ECs may contribute to vascular remodeling, we sought to identify genes regulated by GATA-6. To this end, we used a commercially available EC PCR array (SABiosciences, Valencia, CA) and performed the analyses in HPAECs after

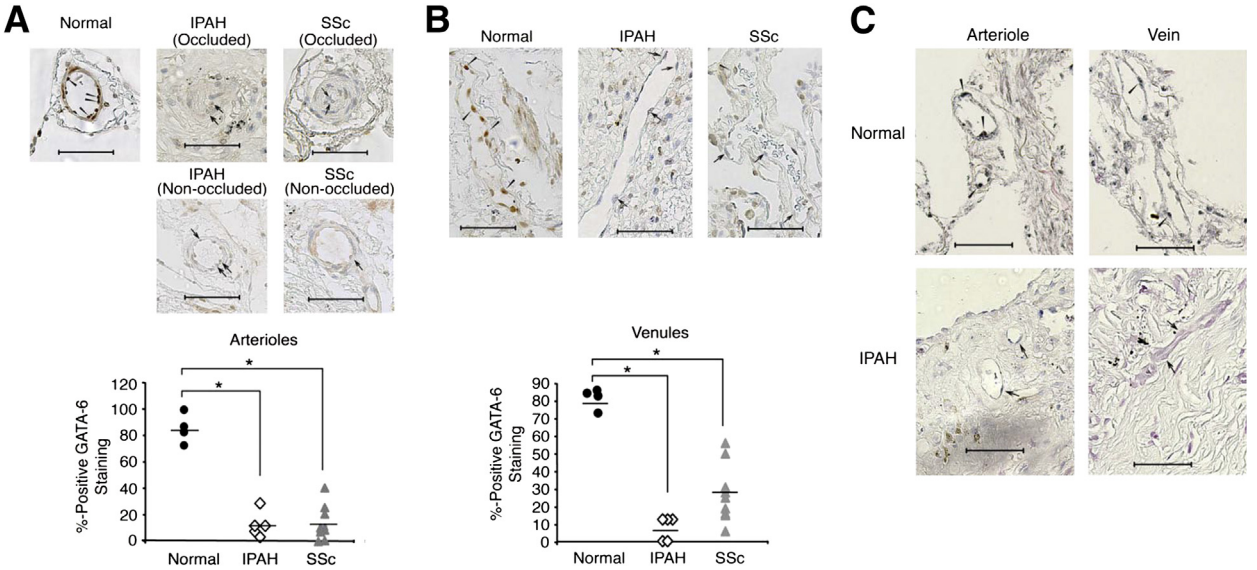

Figure 1 GATA-6 levels are decreased in the pulmonary vasculature of SSc-PAH and IPAH patients. **A** and **B**: Paraffin-embedded tissue sections from four healthy controls, five IPAH, and nine SSc-PAH patients were analyzed for GATA-6 using the standard avidin-biotin-peroxidase methodology. **Arrows** indicate positively or negatively stained ECs in occluded and nonoccluded arterioles (**A**), and venules (**B**) of healthy individuals, IPAH patients, and SSc-PAH patients. **C**: Percentage of positively stained ECs in both occluded and nonoccluded arterioles and venules [in normal (bullets), IPAH (open diamonds) and SSC-PAH (triangles) lung tissues] were plotted on a scatter plot. *$P < 0.01$. *In situ* hybridization of paraffin-embedded tissue from healthy individuals and IPAH patients were used to analyze GATA-6 mRNA levels **Arrows** point to GATA-6 positive or negative ECs in the indicated vessels of healthy controls (**top panel**) or IPAH patients (**bottom panel**). Original magnification, ×400. Scale bars: 50 μm (**A**–**C**).

suppression of GATA-6 with siRNA oligos. This screen identified genes involved in vessel tone and permissibility (*eNOS, ACE, EDNRA, ET-1*), EC activation (*CX3CL1, PAI-1, RhoB,* 5-lipoxygenease-activating protein [*FLAP*]), matrix remodeling (*MMP1, MMP10*), and EC injury (*PLA2G4C*) (for complete list of genes, see Table 4). mRNA levels of putative target genes were examined by RT-qPCR. As shown in Figure 2A, levels of mRNA for PLA2G4C, FLAP, RhoB, MMP1, MMP10, PAI-1, CX3CL1, ACE, EDNRA, and ET-1 were elevated, whereas levels of eNOS were decreased after suppression of GATA-6. Western blot analysis and ELISA also confirmed differential expression of eNOS, MMP-1, MMP-10, PAI-1, RhoB, and CX3CL1 at the protein level (Figure 2, B and C, respectively). These data strongly suggest that GATA-6 may play a role in PAH by regulating genes that promote vascular remodeling and dysfunction. To further investigate if GATA-6 is a direct transcriptional regulator of these genes, we performed chromatin immunoprecipitation analysis. Putative GATA sites were identified using Tfsitescan. As shown in Figure 2D and Table 5, GATA-6 occupied one or more sites on the promoters of FLAP, RhoB, MMP10, MMP1, PAI-1, CX3CL1, eNOS, EDNRA, and ET-1, indicating that GATA-6 is a direct regulator of these genes. We were not able to detect GATA-6 binding on the *PLA2G4C* promoter. Finally, as an additional negative control, we were not able to immunoprecipitate the promoter of VE-Cadherin, a gene that is not regulated by GATA-6 according to our microarray data.

GATA-6 Down-Regulation is an Early Event in the Chronic Hypoxia Mouse Model and the MCT Rat Model of PAH

Because endothelial GATA-6 deficiency affected expression of genes previously implicated in the development of PAH, we next determined the levels of expression of GATA-6 in two rodent models of PAH, the chronic hypoxia mouse model, and the MCT rat model. A significant decrease of Gata-6 expression was already noticeable at 3 days after hypoxia and expression decreased further at 7 and 21 days (Figure 3A). Several of the GATA-6 target genes, including Pla2G4C, RhoB, EDNRA, and Pai-1 were increased, whereas, surprisingly, Cx3cl1 gradually decreased starting at day 3 (Figure 3B). Furthermore, hypoxia inducible factor (Hif) subunits Hif1α, Hif1β, and Hif2α showed the most pronounced upregulation at day 3 (Figure 3B) with significantly elevated levels continuing for the duration of the experiment (up to 2 months) (Supplemental Figure S1).

Next we investigated if Gata-6 expression is decreased after MCT injury (Supplemental Figure S2, A–E). Gata-6 expression was significantly decreased as early as 3 days and further gradually decreased up to 20 days postinjection. Gata-6 protein levels are also decreased in the lung tissue of rats challenged with MCT after 20 days. These findings indicate that GATA-6 expression levels are down-regulated at both early and late stages of disease in two animal models of PAH.

GATA-6 Deficiency Augments mRNA Expression of Endothelial HIF2α and HIF1β

To study the involvement of altered Gata-6 expression in the vasculature *in vivo*, we selectively reduced expression of the Gata-6 gene in ECs by crossing an established, commercially available mouse line harboring a conditional loss-of-function allele of Gata-6 with mice expressing Cre recombinase under the control of the endothelial-specific VE-Cadherin promoter to generate $Gata\text{-}6^{flox/flox}/VEcadCre^{+/-}$ mice (Gata6-KO). Sex-matched littermates lacking the Cre allele were used as controls. Isolation of pulmonary ECs from Gata6-KO mice and controls demonstrated that Gata-6 expression is reduced by 65% (Figure 3C).

After exposure to chronic hypoxia down-regulation of Gata-6 correlated with upregulation of Hif1α and Hifβ and Hif2α, we next assessed the contribution of endothelial Gata-6 to the upregulation of Hif subunits using Wt and Gata6-KO mice. Pulmonary ECs ($CD31^+/CD45^-$) were sorted by FACS at days 1, 3, 5, and 7, and were directly used for mRNA analysis. In Wt mice, a gradual decrease of Gata-6 expression starting at day 1 of hypoxia was observed, whereas a rapid increase of Hif1α occurred at day1, then gradually returned to control levels by day 7 (Figure 3D). A similar pattern of expression was also observed for Hif1β and Hif2α. These data suggest that ECs may contribute to the initial upregulation, but not to the prolonged activation of Hif genes in response to hypoxia. Interestingly, pulmonary ECs isolated from Gata6-KO mice showed increased baseline expression of Hif1α and Hif1β, as well as Hif2α. Similar to Wt mice, a further transient increase of Hif gene expression was observed in Gata6-KO ECs. The Gata-6 mRNA levels in Gata6-KO mice were comparable to the levels in Wt mice. To determine whether GATA-6 could directly contribute to the upregulation of HIF genes, HIF1α, Hif1β, and HIF2α were analyzed in HPAECs after suppression of GATA-6 with siRNA oligos. As shown in Figure 3E, expression of HIF1β and HIF2α was significantly increased, whereas expression of HIF1α remained unchanged after depletion of GATA-6. Together, these data suggest that absence of endothelial GATA-6 may exacerbate effects of hypoxia in pulmonary vasculature.

GATA-6 Deficiency Leads to Elevated Pulmonary Arterial Pressure

At 12 weeks of age, mice were subjected to echocardiographical imaging before and after exposure to chronic hypoxia. Using pulsed-wave Doppler of PA flow, PAT, and ejection time were measured (Figure 4A). This noninvasive assessment of PAH has been validated in mice as a sensitive method to assess changes in RV systolic pressure.[28] Gata6-KO mice had significantly lower PAT at baseline compared to Wt, which lowered significantly more after exposure to

Table 4 The Human Endothelial Cell Biology RT^2 *Profiler* PCR Array Gene List

		Up-regulation and down-regulation (compared to control group)
		Group 1
Description	Symbol	Fold regulation
Angiotensin I converting enzyme (peptidyl-dipeptidase A) 1	*ACE*	2.3457
ADAM metallopeptidase domain 17	*ADAM17*	1.2746
Angiotensinogen (serpin peptidase inhibitor, clade A, member 8)	*AGT*	−1.014
Angiotensin II receptor, type 1	*AGTR1*	−1.014
Arachidonate 5-lipoxygenase	*ALOX5*	1.954
Angiopoietin 1	*ANGPT1*	−1.014
Annexin A5	*ANXA5*	1.0425
BCL2-associated X protein	*BAX*	−1.1647
B-cell CLL/lymphoma 2	*BCL2*	−1.3566
BCL2-related protein A1	*BCL2A1*	1.454
BCL2-like 1	*BCL2L1*	1.5801
Chemokine (C-X-C motif) receptor 5	*CXCR5*	−1.014
Caspase 1, apoptosis-related cysteine peptidase (interleukin 1, beta, convertase)	*CASP1*	−1.0281
Caspase 3, apoptosis-related cysteine peptidase	*CASP3*	1.007
Caspase 6, apoptosis-related cysteine peptidase	*CASP6*	1.1728
Chemokine (C-C motif) ligand 2	*CCL2*	1.3379
Chemokine (C-C motif) ligand 5	*CCL5*	−1.0644
Cadherin 5, type 2 (vascular endothelium)	*CDH5*	1.1173
CASP8 and FADD-like apoptosis regulator	*CFLAR*	1.3104
Collagen, type XVIII, alpha 1	*COL18A1*	1.2834
Carboxypeptidase B2 (plasma)	*CPB2*	2.941
CASP2 and RIPK1 domain containing adaptor with death domain	*CRADD*	2.0705
Colony stimulating factor 2 (granulocyte-macrophage)	*CSF2*	−1.014
Chemokine (C-X3-C motif) ligand 1	*CX3CL1*	2.7895
Thymidine phosphorylase	*TYMP*	1.3472
Endothelin 1	*EDN1*	1.4044
Endothelin 2	*EDN2*	−1.014
Endothelin receptor type A	*EDNRA*	2.395
Fas (TNF receptor superfamily, member 6)	*FAS*	−1.1019
Fas ligand (TNF superfamily, member 6)	*FASLG*	−1.014
Fibroblast growth factor 1 (acidic)	*FGF1*	−1.014
Fms-related tyrosine kinase 1 (vascular endothelial growth factor/vascular permeability factor receptor)	*FLT1*	1.1408
Fibronectin 1	*FN1*	1.5263
Intercellular adhesion molecule 1	*ICAM1*	1.434
Interferon, beta 1, fibroblast	*IFNB1*	1.7654
Interleukin 11	*IL11*	1.7901
Interleukin 1, beta	*IL1B*	1.5134
Interleukin 3 (colony-stimulating factor, multiple)	*IL3*	−1.014
Interleukin 6 (interferon, beta 2)	*IL6*	−1.1408
Interleukin 7	*IL7*	−1.1567
Integrin, alpha 5 (fibronectin receptor, alpha polypeptide)	*ITGA5*	1.2834
Integrin, alpha V (vitronectin receptor, alpha polypeptide, antigen CD51)	*ITGAV*	1.0425
Integrin, beta 1 (fibronectin receptor, beta polypeptide, antigen CD29 includes MDF2, MSK12)	*ITGB1*	1
Integrin, beta 3 (platelet glycoprotein IIIa, antigen CD61)	*ITGB3*	−1.2924
Kinase insert domain receptor (a type III receptor tyrosine kinase)	*KDR*	1.2658
V-kit Hardy-Zuckerman 4 feline sarcoma viral oncogene homolog	*KIT*	−1.0867
Kallikrein-related peptidase 3	*KLK3*	−1.014
Matrix metallopeptidase 1 (interstitial collagenase)	*MMP1*	2.0705
Matrix metallopeptidase 2 (gelatinase A, 72kDa gelatinase, 72kDa type IV collagenase)	*MMP2*	1.2658
Matrix metallopeptidase 9 (gelatinase B, 92kDa gelatinase, 92kDa type IV collagenase)	*MMP9*	3.7412
Nitric oxide synthase 2, inducible	*NOS2*	1.2658
Nitric oxide synthase 3 (endothelial cell)	*NOS3*	−2.3134

(*table continues*)

Table 4 (*continued*)

Description	Up-regulation and down-regulation (compared to control group)	
		Group 1
	Symbol	Fold regulation
Natriuretic peptide B	*NPPB*	−1.014
Natriuretic peptide receptor A/guanylate cyclase A (atrionatriuretic peptide receptor A)	*NPR1*	1.1329
Occludin	*OCLN*	−1.014
Platelet-derived growth factor receptor, alpha polypeptide	*PDGFRA*	1.9211
Platelet/endothelial cell adhesion molecule	*PECAM1*	1.1567
Platelet factor 4	*PF4*	−1.0425
Placental growth factor	*PGF*	1.0867
Phospholipase A2, group IVC (cytosolic, calcium-independent)	*PLA2G4C*	1.8703
Plasminogen activator, tissue	*PLAT*	1.4845
Plasminogen activator, urokinase	*PLAU*	1.5476
Plasminogen	*PLG*	−1.014
Prostaglandin I2 (prostacyclin) synthase	*PTGIS*	−1.5443
Ras homolog gene family, member B	*RHOB*	1.7443
Receptor (TNFRSF)-interacting serine-threonine kinase 1	*RIPK1*	1.0497
Selectin E	*SELE*	−1.1251
Selectin L	*SELL*	−1.9754
Selectin P ligand	*SELPLG*	−1.014
Serpin peptidase inhibitor, clade E (nexin, plasminogen activator inhibitor type 1), member 1	*SERPINE1*	2.2658
Superoxide dismutase 1, soluble	*SOD1*	1.0353
Sphingosine kinase 1	*SPHK1*	1.2483
TEK tyrosine kinase, endothelial	*TEK*	1.1567
Tissue factor pathway inhibitor (lipoprotein-associated coagulation inhibitor)	*TFPI*	−1.0943
Thrombomodulin	*THBD*	−1.1251
Thrombospondin 1	*THBS1*	1.3013
TIMP metallopeptidase inhibitor 1	*TIMP1*	−1.1096
Tumor necrosis factor	*TNF*	−1.014
Tumor necrosis factor, α-induced protein 3	*TNFAIP3*	1.4044
Tumor necrosis factor receptor superfamily, member 10c, decoy without an intracellular domain	*TNFRSF10C*	−1.0792
Tumor necrosis factor (ligand) superfamily, member 10	*TNFSF1*	−1.2397
Vascular cell adhesion molecule 1	*VCAM1*	1.2397
Vascular endothelial growth factor A	*VEGFA*	1.7171
Von Willebrand factor	*VWF*	1.1567
Beta-2-microglobulin	*B2 mol/L*	−1.2142
Hypoxanthine phosphoribosyltransferase 1	*HPRT1*	1.1173
Ribosomal protein L13a	*RPL13A*	−1.0281
Glyceraldehyde-3-phosphate dehydrogenase	*GAPDH*	1.1173
Actin, beta	*ACTB*	1.5052
Human genomic DNA contamination	*HGDC*	−1.014
Reverse transcription control	*RTC*	1.2658
Reverse transcription control	*RTC*	1.257
Reverse transcription control	*RTC*	1.3379
Positive PCR control	*PPC*	1.0497
Positive PCR control	*PPC*	−1.4743
Positive PCR control	*PPC*	−1.2658

ADAM, A-disintegrin and metalloproteinase; BCL2, B cell lymphoma 2; CASP8, cysteine-aspartic protease 8; CLL, chronic lymphoid leukemia; FADD, fas-associated protein with death domain; TEK, tyrosine kinase endothelial; TIMP, tissue inhibitor of metalloproteinases; TNF, tumor necrosis factor.

hypoxia for 2 months (Supplemental Figure S3). PAT was decreased in Wt after exposure to chronic hypoxia, indicative of PAH. PAT/ejection time was also lower in Gata6-KO than Wt under normoxic conditions and significantly lower in both Wt and Gata6-KO mice after hypoxic insult for 1 and 2 months. To confirm the presence of increased PA pressure among Gata6-KO mice, we also performed right heart catheterization (Figure 4B). RV systolic pressure was significantly elevated in Gata6-KO mice compared to Wt mice at baseline, and significantly increased in both Wt and Gata6-KO mice after exposure to hypoxia for 1 month.

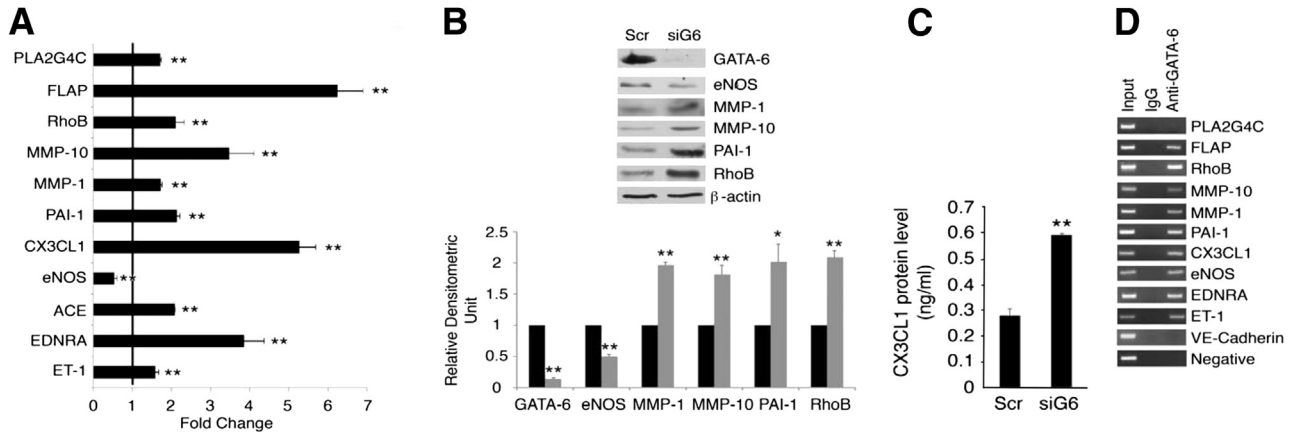

Figure 2 GATA-6 regulates genes involved in vascular remodeling. HPAECs were transfected with control or small interfering RNA against GATA-6 oligos for 72 hours. Samples were assayed by RT-qPCR to determine mRNA levels (**A**) or by Western blot analysis (**B**) and ELISA (**C**) to determine protein levels for the genes indicated. The experiments were performed at least three times and representative blots are shown. Band intensities were quantified by densitometric analysis. Black bars, control siRNA; grey bars, Gata6 siRNA treated cells. $*P < 0.05$, $**P < 0.01$. **D:** Chromatin immunoprecipitation assays were performed in HPAECs using rabbit anti—GATA-6 polyclonal antibody or rabbit IgG. The experiments were performed at least three times and representative gels are shown.

Systolic blood pressure, diastolic blood pressure, mean pressure, heart pulse rate, and blood volume appeared to be no different in the Gata6-KO mice (Table 6). Heart morphology was investigated by serially sectioning hearts from both Wt and Gata6-KO mice housed in both hypoxic and normoxic conditions. There were no observed defects in valve morphology in Gata6-KO mice in comparison to Wt controls. Furthermore, there was no evidence of intramyocardial shunting of blood, as there were no detectable septal defects in Gata6-KO mice in either hypoxic or normoxic conditions. Myocardial histology also appeared normal (Supplemental Figure S4).

We concluded from these experiments that a reduction of Gata-6 alone is enough to alter the PA pressure in mice and that loss of Gata-6 leads to more severe changes in hemodynamics under hypoxia.

GATA-6 Deficiency Leads to Worsened Vascular Remodeling and RV Hypertrophy in Hypoxic Mice

To investigate the effect of decreased Gata-6 levels on pulmonary vascular remodeling, the degree of muscularization and the medial wall thickness of intra-acinar PAs (20

Table 5 Summary of Results for ChIP Analysis

Gene	Predicted putative GATA binding site	Amplified regions of target gene promoter	*In vivo* binding of GATA-6
PLA2G4C	−982 to 977, −962 to 957	−1081 to 878	+
FLAP	−1101 to 1096	−1134 to 966	+
RhoB	−1877 to 1872, −1731 to 1726,	−1908 to 1689	+
	−862 to 857	−1034 to 801	−
MMP-10	−1831 to 1826, −1798 to 1793	−1922 to 1721	+
	−1573 to 1568	−1650 to 1428	−
	−994 to 989	−1112 to 885	−
	−226 to 221	−270 to 114	+
MMP-1	−1356 to 1351, −1323 to 1318	−1435 to 1200	+
	−1112 to 1107, −982 to 977, −955 to 950	−1137 to 907	−
PAI-1	−1691 to 1686	−1739 to 1556	+
	−572 to 567	−677 to 490	+
	−431 to 426	−510 to 305	+
CX3CL1	−881 to 876, −801 to 796	−958 to 755	+
eNOS	−1114 to 1109	−1220 to 1000	−
	−203 to 198	−300 to 119	+
EDNRA	−767 to 762	−846 to 650	−
	−495 to 490	−568 to 421	−
	−328 to 323	−420 to 261	+
ET-1	−1207 to 1202, −1154 to 1149	−1298 to 1107	−
	−745 to 740, −701 to 696, −681 to 676	−849 to 652	−
	−136 to 131	−254 to 68	+

ChIP, chromatin immunoprecipitation.

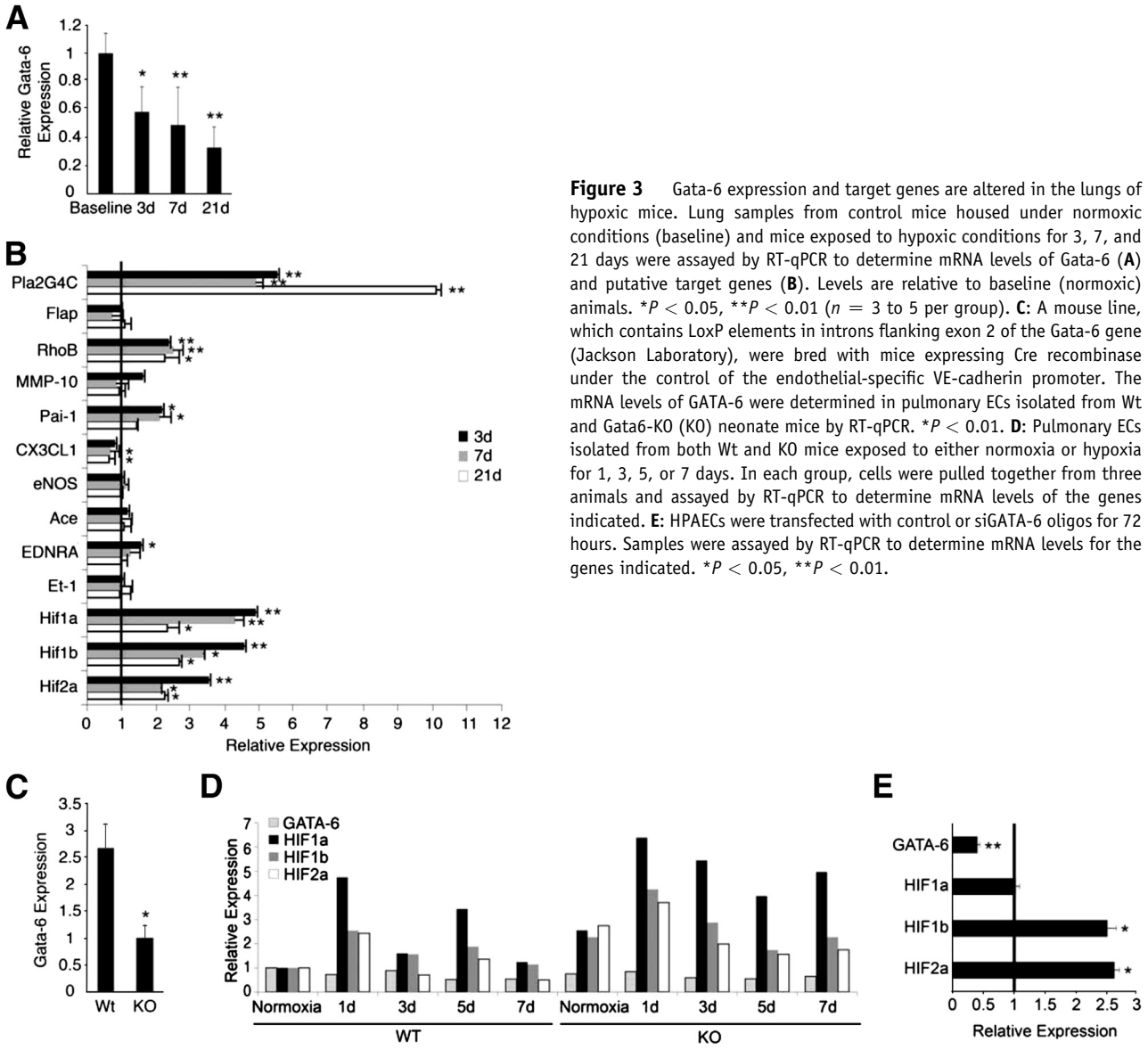

Figure 3 Gata-6 expression and target genes are altered in the lungs of hypoxic mice. Lung samples from control mice housed under normoxic conditions (baseline) and mice exposed to hypoxic conditions for 3, 7, and 21 days were assayed by RT-qPCR to determine mRNA levels of Gata-6 (**A**) and putative target genes (**B**). Levels are relative to baseline (normoxic) animals. $*P < 0.05$, $**P < 0.01$ ($n = 3$ to 5 per group). **C:** A mouse line, which contains LoxP elements in introns flanking exon 2 of the Gata-6 gene (Jackson Laboratory), were bred with mice expressing Cre recombinase under the control of the endothelial-specific VE-cadherin promoter. The mRNA levels of GATA-6 were determined in pulmonary ECs isolated from Wt and Gata6-KO (KO) neonate mice by RT-qPCR. $*P < 0.01$. **D:** Pulmonary ECs isolated from both Wt and KO mice exposed to either normoxia or hypoxia for 1, 3, 5, or 7 days. In each group, cells were pulled together from three animals and assayed by RT-qPCR to determine mRNA levels of the genes indicated. **E:** HPAECs were transfected with control or siGATA-6 oligos for 72 hours. Samples were assayed by RT-qPCR to determine mRNA levels for the genes indicated. $*P < 0.05$, $**P < 0.01$.

to 70 μm in diameter) were analyzed in normoxic and hypoxic conditions. Morphometric analysis revealed a significant difference between Gata6-KO mice and control animals under both conditions. Furthermore, severe enhanced PA muscularization seen by enhanced immunoreactivity for α-SMA actin was observed in Gata6-KO mice subjected to hypoxia for 1 month (Figure 5A). The analysis revealed significantly more fully and partially muscularized vessels in the Gata6-KO mice and less nonmuscularized vessels (Figure 5B). Under hypoxia, Gata6-KO mice had an even more dramatic increase in fully muscularized vessels, as well as a marked decrease in nonmuscularized vessels. In addition, the medial wall thickness was significantly increased in Gata6-KO mice under hypoxic conditions (Figure 5C). Finally, we observed that Gata-6-KO hypoxic mice also had significantly larger right ventricles as evidenced by an increase in the ratio of RV to left ventricular (LV) plus septum weight (RV/[LV+S]) as compared to control littermates (Figure 5D).

GATA-6 Deficiency Induces Pathological Changes in Pulmonary Gene Expression *in Vivo*

Next we analyzed the levels of GATA-6 target genes found earlier in HPAECs (Figure 2) in the lungs of Gata6-KO and control animals under both normoxic and hypoxic conditions. Under normoxia, the pattern of gene expression in the Gata-6 KO mice largely reproduced that of GATA-6-deficient HPAECs (Figure 6A). In particular, expression of CX3CL1 and EDNRA was significantly increased. Changes in expression of other genes did not reach statistical significance, likely due to variability between the mice and a small number of mice in each group ($n = 3$ to 4); however, they showed the same trends as HPAECs, with the exception of matrix metalloproteinase 10 and 5-lipoxygenase activating protein, which did not change in the Gata6-KO mice. Several of the GATA-6 target genes, including Pla2G4C, RhoB, EDNRA, and ET-1 were also upregulated in

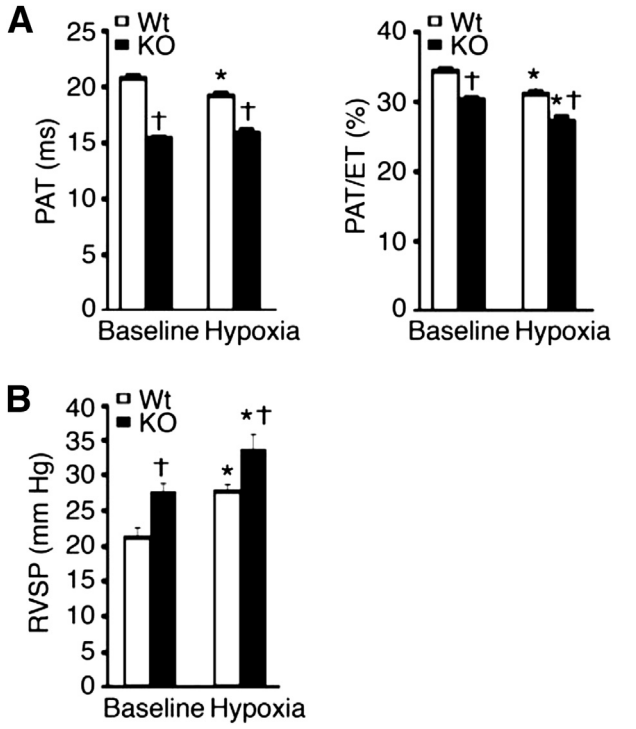

Figure 4 GATA-6 deficiency induces hemodynamic changes in mice. Pulmonary acceleration time (PAT) and PAT as a fraction of ejection time (PAT/ET) (**A**) and RV systolic pressure (RVSP) (**B**) were measured in Wt and Gata6-KO (KO) mice during normoxia (baseline) and after 1 month of chronic hypoxia (see *Materials and Methods*). $^{*}P < 0.05$ versus baseline; $^{\dagger}P < 0.05$ versus Wt. $n = 3$ to 4 per group.

Wt mice exposed to 1 month of hypoxia and were further increased in hypoxic Gata6-KO mice (Figure 6B). A significant increase of RhoB and PAI-1 was observed after 2 months of hypoxia in Wt mice, and an even more pronounced increase of those genes was observed in Gata-6-KO mice (Supplemental Figure S1). Hif1α and Hif1β were modestly elevated in normoxic Gata-6-KO mice, whereas expression of all three factors was significantly increased in Wt and Gata-6-KO mice after 1 and 2 months of hypoxia (Figure 6B and Supplemental Figure S1). Notably, expression of Cx3cl1 gene was significantly reduced in hypoxic Wt mice in comparison to Wt mice from normoxic conditions and was also less prominently increased in Gata6-KO mice from the hypoxic conditions as compared to normoxia. Although, only a limited number of genes have been analyzed, these data suggest that the mechanisms of the vascular injury induced by hypoxia share both common and distinct pathways with those regulated by GATA-6.

Table 6 Occlusion Tail-Cuff Measurements

Animal	SBP	DBP	Mean BP	HR	Volume
Wt 1	92	67	74	628	27
Wt 2	107	79	88	674	39
Wt 3	108	79	89	454	32
Wt 4	82	59	66	606	30
KO 1	76	50	59	488	27
KO 2	92	69	76	666	34
KO 3	80	49	59	519	29
KO 4	130	111	117	702	33

BP, blood pressure; DBP, diastolic blood pressure; HR, heart rate; KO, Gata6-KO; SBP, systolic blood pressure; Wt, wild-type.

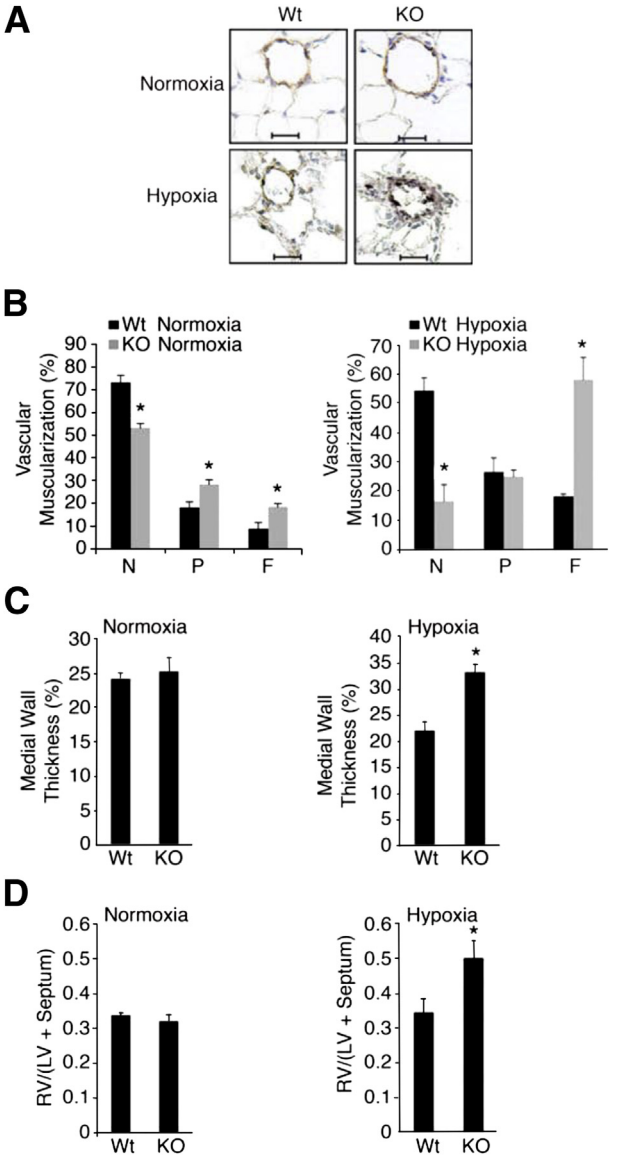

Figure 5 Loss of GATA-6 leads to worsened vessel muscularization and RV hypertrophy in mice exposed to hypoxia. **A:** Lungs and hearts from 12- to 16-week-old male Wt and Gata6-KO (KO) mice exposed to either normoxic or hypoxic conditions for 1 month were subjected to morphometric analysis of pulmonary vessels and RV hypertrophy measurements. Lung sections were stained for von Willebrand factor (brown) and α-SMA (purple). Representative microphotographs are shown. Original magnification, ×400. Scale bars: 20 μm. **B:** Morphometry was performed on the double immunostained lung sections. A total of 60 to 80 intra-acinar vessels ranging in 20 to 70 μm in size were counted and categorized into nonmuscularized (N), partially (P) muscularized, or fully (F) muscularized (see *Materials and Methods*). $^{*}P < 0.01$. **C:** Percent wall thickness was measured in round fully muscularized PAs (see *Materials and Methods*). **D:** The weight ratios of the right ventricle to the left ventricle plus septum [RV/(LV + Septum)] were calculated as indices of RV hypertrophy. $^{*}P < 0.05$.

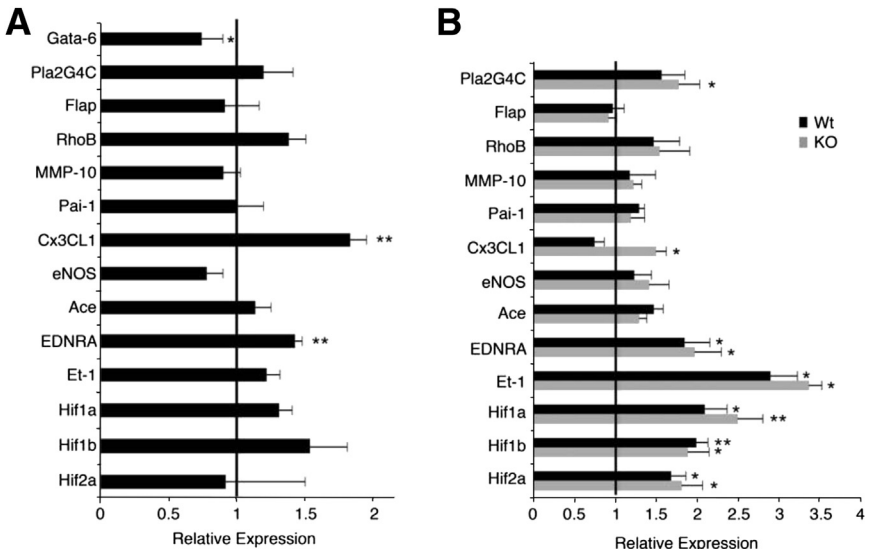

Figure 6 **A**: Gata-6 regulates genes involved in vessel remodeling *in vivo*. Lung samples from Gata6-KO (KO) mice and controls were assayed by RT-qPCR to determine mRNA levels of putative target genes. **B**: Lung samples from KO and control Wt mice subjected to hypoxic conditions for 1 month were assayed by RT-qPCR to determine mRNA levels of Gata-6 target genes relative to control Wt mice housed in normoxic conditions. $*P < 0.05$, $**P < 0.01$. $n = 3$ to 5 per group.

GATA-6 Deficient Mice Show Persistent Inflammation *in Vivo*

Given the persistently elevated expression of Cx3cl1 in Gata6-KO mice, we sought to determine whether recruitment of inflammatory cells to pulmonary vasculature is affected in these mice. FACS analysis was performed on lung tissues from Wt and Gata-6-KO mice in normoxic conditions and after 1 month of hypoxia challenge. The number of T cells ($CD3^+/CD45^+$) and B cells ($B220^+/CD45^+$) was similar in Wt and Gata-6-KO mice under normoxia and was similarly increased in both strains under hypoxia (Figure 7A). In contrast, macrophages ($CD11b^+/F4/80^+$), granulocytes ($Ly6G^+/CD45^+$), and dendritic cells ($CD11b^+/CD11c^+$) were significantly increased in Gata-6-KO mice under normoxic conditions, but did not differ significantly in hypoxic mice (Figure 7A). An increased presence of monocytes/macrophages in Gata6-KO mice was further confirmed in lung tissue sections from Wt and Gata6-KO mice (Figure 7B).

Discussion

All forms of PAH are characterized by severe pulmonary vascular remodeling that leads to increased vascular resistance and ultimately right heart failure. The molecular mechanisms underlying the remodeling process and especially early pathogenic changes in the EC compartment remain elusive. Herein, we show that down-regulation of GATA-6 in ECs represents a key pathological event during development of PAH. GATA-6 is reduced in ECs, as well as smooth muscle cells of both occluded and nonoccluded pulmonary vessels of both IPAH and SSc-PAH *in vivo*, suggesting that reduction of GATA-6 is not a consequence of late stage vessel remodeling, but occurs before vessel occlusion and may reflect an early phase of EC activation and/or dysfunction during PAH. This notion is supported by observations from the two animal models of PAH, the MCT rat model and the chronic hypoxia mouse model, that show rapid reduction of the GATA-6 mRNA levels in the lungs after injury (at 3 days). Regulatory pathways that are involved in GATA-6 down-regulation remain to be elucidated.

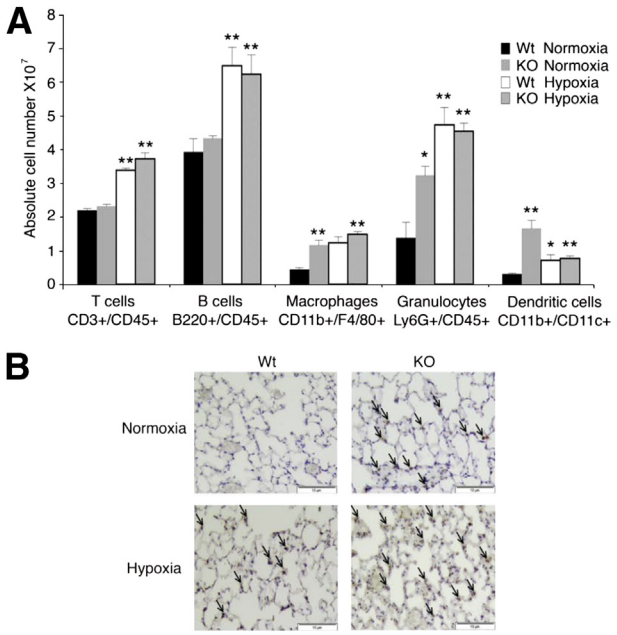

Figure 7 Gata-6 (KO) deficiency leads to increased perivascular inflammation. **A**: Single cell suspensions isolated from Wt and KO mice exposed to both normoxia and hypoxia for 1 month were stained with fluorochrome-conjugated antibodies for the indicated cell surface proteins and subjected to flow cytometry analysis. $*P < 0.05$, $**P < 0.01$. **B**: Lung sections from Wt and KO mice exposed to normoxic or hypoxic conditions for 2 months were subjected to immunostaining for Mac3 using the standard avidin-biotin-peroxidase methodology. Immunoreactivity was detected using 3, 3′-diaminiobenzidine substrate kit. Hematoxylin was used as a counterstain. **Arrows** indicate positively stained macrophages. Original magnification, ×200. Scale bars: 10 μm.

Characterization of Gata6-KO mice revealed that GATA-6 is particularly important for pulmonary hemodynamics because a loss of GATA-6 alone was sufficient to raise PA pressure, but not systemic blood pressure. This may be due, in part, to enhanced vasoconstriction caused by changes in the levels of regulators of vascular tone (eNOS and ET-1). The eNOS null mice develop mild PAH under normoxic conditions and severe PAH under slightly hypoxic conditions.[29] Impaired bioavailability of active nitric oxide is a major underlying feature of most clinical and experimental forms of PAH.[30] Furthermore, ET-1, as well as endothelin-1 receptor type A, was significantly increased after down-regulation of GATA-6 by siRNA in cultured HPAECs and in Gata6-KO mice. ET-1 is a potent vasoconstrictor, a mitogen for pulmonary VSMCs, and a fibrogenic mediator.[31] Plasma levels of ET-1 are elevated in PAH and are inversely proportional to the levels of pulmonary blood flow and cardiac output.[32,33] Moreover, a recent study has linked EDNRA polymorphism to an increased susceptibility to PAH.[34]

Evidence suggests that inflammatory events may contribute to the pathogenesis of various forms of PAH, including IPAH and SSc-PAH.[35,36] It has also been suggested that inflammatory pathways and autoimmunity play a more prominent role in SSc-PAH versus IPAH and may contribute to the differential response to therapy between the two syndromes.[37] This study identified CX3CL1 (fractalkine) as one of the GATA-6 direct target genes. To our knowledge, this is the first demonstration that GATA-6 functions as a transcriptional repressor of the CX3CL1 gene. Elevated levels of fractalkine have been observed in inflammatory lung diseases including chronic obstructive pulmonary disease and PAH.[38] Fractalkine was also found in the top 20 most upregulated genes in SSc-PAH by a recent microarray analysis.[10] In human PAH, ECs were found to be the main source of CX3CL1 in the PA.[39] In addition to recruiting inflammatory cells, CX3CL1 has been shown to act as a mitogenic agent on VSMCs in atherosclerosis[40] and as an inducer of angiogenesis via stimulation of HIF-1α/vascular endothelial growth factor-A axis,[41] suggesting that fractalkine may regulate various pathological aspects of PAH. Interestingly, although Gata-6 expression was reduced in hypoxia in Wt mice, we also observed concomitant reduction of Cx3cl1, suggesting that hypoxia-driven pathways supersede the effect of Gata-6 down-regulation. These findings corroborate an earlier *in vitro* study that demonstrated hypoxia-mediated inhibition of interferon-γ-induced Cx3cl1 in ECs.[42]

In addition to its effect on fractalkine expression, GATA-6 may regulate cytokine release by directly controlling expression of FLAP, which activates 5-lipooxygenase. It is possible that 5-lipooxygenase plays an early role in triggering a pro-inflammatory environment because its activation and translocation to the nuclear membrane are required for the production of leukotrienes, which are known to induce cytokine release.[43] Both 5-lipooxygenase and FLAP have been shown to be upregulated in PAs of IPAH patients, and inhibition of FLAP in hypoxic rats ameliorates pulmonary hypertension and vascular reactivity.[44,45]

A reduction of Gata-6 alone significantly altered the PA pressure in mice, and increased vascular remodeling and infiltration of inflammatory cells under basal conditions. Perivascular inflammation is present in other animal models of PAH and in human PAH, however, the role of inflammatory cells in the disease process is not yet clear.[46] It is important to note that in our model, Gata-6 was deleted from ECs only, whereas in patients with PAH, both endothelial and smooth muscle cells were deficient for GATA-6. Also, GATA-6 may have a distinct role in endothelial and smooth muscle cells, and its absence in both cell types would likely result in a more severe phenotype. As shown herein, Gata-6 expression in ECs was gradually decreased after treatment of mice with chronic hypoxia, suggesting that hypoxic conditions may be in part responsible for the changes in Gata-6 levels in patients with PAH. Further studies are needed to determine whether GATA-6 is also regulated by hypoxia in smooth muscle cells.

In SSc, endothelial injury resulting in the structural changes in the microvasculature and autoimmunity are the earliest manifestations of the disease.[47] Although PAH develops only in a subset of patients, survival of SSc-PAH patients is very poor as compared to IPAH.[9] In addition to pulmonary vessels, we have also observed decreased levels of GATA-6 in the dermis of the majority of SSc patients (Ghatnekar and Trojanowska, unpublished data) supporting the notion that chronic systemic changes in the vasculature occurring in various organs may be the principal reason for the differences in survival between these two diseases. In conclusion, we describe a novel model of PAH characterized by EC injury and persistent inflammation that may provide new insights into the role of endothelial-immune axis during development of PAH. We believe that this new model will be particularly informative in dissecting the mechanisms involved in SSc-PAH.

Supplemental Data

Supplemental material for this article can be found at *http://dx.doi.org/10.1016/j.ajpath.2013.02.039*.

References

1. Simonneau G, Robbins IM, Beghetti M, Channick RN, Delcroix M, Denton CP, Elliott CG, Gaine SP, Gladwin MT, Jing ZC, Krowka MJ, Langleben D, Nakanishi N, Souza R: Updated clinical classification of pulmonary hypertension. J Am Coll Cardiol 2009, 54:S43−S54
2. Fisher MR, Mathai SC, Champion HC, Girgis RE, Housten-Harris T, Hummers L, Krishnan JA, Wigley F, Hassoun PM: Clinical differences between idiopathic and scleroderma-related pulmonary hypertension. Arthritis Rheum 2006, 54:3043−3050
3. Chan SY, Loscalzo J: Pathogenic mechanisms of pulmonary arterial hypertension. J Mol Cell Cardiol 2008, 44:14−30
4. The International PPH Consortium, Lane KB, Machado RD, Pauciulo MW, Thomson JR, Phillips JA, 3rd, Loyd JE, Nichols WC, Trembath RC: Heterozygous germline mutations in BMPR2, encoding a TGF-beta receptor, cause familial primary pulmonary hypertension. Nat Genet 2000, 26:81−84
5. Mahmoud M, Borthwick GM, Hislop AA, Arthur HM: Endoglin and activin receptor-like-kinase 1 are co-expressed in the distal vessels of

the lung: implications for two familial vascular dysplasias, HHT and PAH. Lab Invest 2009, 89:15–25
6. Hong KH, Lee YJ, Lee E, Park SO, Han C, Beppu H, Li E, Raizada MK, Bloch KD, Oh SP: Genetic ablation of the BMPR2 gene in pulmonary endothelium is sufficient to predispose to pulmonary arterial hypertension. Circulation 2008, 118:722–730
7. Morse J, Barst R, Horn E, Cuervo N, Deng Z, Knowles J: Pulmonary hypertension in scleroderma spectrum of disease: lack of bone morphogenetic protein receptor 2 mutations. J Rheumatol 2002, 29: 2379–2381
8. Selva-O'Callaghan A, Balada E, Serrano-Acedo S, Simeon Aznar CP, Ordi-Ros J: Mutations of activin-receptor-like kinase 1 (ALK-1) are not found in patients with pulmonary hypertension and underlying connective tissue disease. Clin Rheumatol 2007, 26:947–949
9. Le Pavec J, Humbert M, Mouthon L, Hassoun PM: Systemic sclerosis-associated pulmonary arterial hypertension. Am J Respir Crit Care Med 2010, 181:1285–1293
10. Hsu E, Shi H, Jordan RM, Lyons-Weiler J, Pilewski JM, Feghali-Bostwick CA: Lung tissues in patients with systemic sclerosis have gene expression patterns unique to pulmonary fibrosis and pulmonary hypertension. Arthritis Rheum 2011, 63:783–794
11. Molkentin JD: The zinc finger-containing transcription factors GATA-4, -5, and -6. Ubiquitously expressed regulators of tissue-specific gene expression. J Biol Chem 2000, 275:38949–38952
12. Suzuki E, Evans T, Lowry J, Truong L, Bell DW, Testa JR, Walsh K: The human GATA-6 gene: structure, chromosomal location, and regulation of expression by tissue-specific and mitogen-responsive signals. Genomics 1996, 38:283–290
13. Nishida W, Nakamura M, Mori S, Takahashi M, Ohkawa Y, Tadokoro S, Yoshida K, Hiwada K, Hayashi K, Sobue K: A triad of serum response factor and the GATA and NK families governs the transcription of smooth and cardiac muscle genes. J Biol Chem 2002, 277:7308–7317
14. Wada H, Hasegawa K, Morimoto T, Kakita T, Yanazume T, Sasayama S: A p300 protein as a coactivator of GATA-6 in the transcription of the smooth muscle-myosin heavy chain gene. J Biol Chem 2000, 275:25330–25335
15. Mano T, Luo Z, Malendowicz SL, Evans T, Walsh K: Reversal of GATA-6 downregulation promotes smooth muscle differentiation and inhibits intimal hyperplasia in balloon-injured rat carotid artery. Circ Res 1999, 84:647–654
16. Ghatnekar A, Trojanowska M: GATA-6 is a novel transcriptional repressor of the human Tenascin-C gene expression in fibroblasts. Biochim Biophys Acta 2008, 1779:145–151
17. Cowan KN, Jones PL, Rabinovitch M: Elastase and matrix metalloproteinase inhibitors induce regression, and tenascin-C antisense prevents progression, of vascular disease. J Clin Invest 2000, 105:21–34
18. Kubo M, Umemoto S, Fujii K, Itoh S, Tanaka M, Kawahara S, Matsuzaki M: Effects of angiotensin II type 1 receptor antagonist on smooth muscle cell phenotype in intramyocardial arteries from spontaneously hypertensive rats. Hypertens Res 2004, 27:685–693
19. Liu B, Wang XQ, Yu L, Zhou TF, Wang XM, Liu HM: Simvastatin restores down-regulated GATA-6 expression in pulmonary hypertensive rats. Exp Lung Res 2009, 35:411–426
20. Froese N, Kattih B, Breitbart A, Grund A, Geffers R, Molkentin JD, Kispert A, Wollert KC, Drexler H, Heineke J: GATA6 promotes angiogenic function and survival in endothelial cells by suppression of autocrine transforming growth factor beta/activin receptor-like kinase 5 signaling. J Biol Chem 2011, 286:5680–5690
21. Giusti B, Fibbi G, Margheri F, Serrati S, Rossi L, Poggi F, Lapini I, Magi A, Del Rosso A, Cinelli M, Guiducci S, Kahaleh B, Bazzichi L, Bombardieri S, Matucci-Cerinic M, Gensini GF, Del Rosso M, Abbate R: A model of anti-angiogenesis: differential transcriptosome profiling of microvascular endothelial cells from diffuse systemic sclerosis patients. Arthritis Res Ther 2006, 8:R115
22. Wirrig EE, Snarr BS, Chintalapudi MR, O'Neal JL, Phelps AL, Barth JL, Fresco VM, Kern CB, Mjaatvedt CH, Toole BP, Hoffman S, Trusk TC, Argraves WS, Wessels A: Cartilage link protein 1 (Crtl1), an extracellular matrix component playing an important role in heart development. Dev Biol 2007, 310:291–303
23. Shirasaki F, Makhluf HA, LeRoy C, Watson DK, Trojanowska M: Ets transcription factors cooperate with Sp1 to activate the human tenascin-C promoter. Oncogene 1999, 18:7755–7764
24. Nakerakanti SS, Kapanadze B, Yamasaki M, Markiewicz M, Trojanowska M: Fli1 and Ets1 have distinct roles in connective tissue growth factor/CCN2 gene regulation and induction of the profibrotic gene program. J Biol Chem 2006, 281:25259–25269
25. Summer R, Fiack CA, Ikeda Y, Sato K, Dwyer D, Ouchi N, Fine A, Farber HW, Walsh K: Adiponectin deficiency: a model of pulmonary hypertension associated with pulmonary vascular disease. Am J Physiol Lung Cell Mol Physiol 2009, 297:L432–L438
26. Steudel W, Ichinose F, Huang PL, Hurford WE, Jones RC, Bevan JA, Fishman MC, Zapol WM: Pulmonary vasoconstriction and hypertension in mice with targeted disruption of the endothelial nitric oxide synthase (NOS 3) gene. Circ Res 1997, 81:34–41
27. Morrell NW, Adnot S, Archer SL, Dupuis J, Jones PL, MacLean MR, McMurtry IF, Stenmark KR, Thistlethwaite PA, Weissmann N, Yuan JX, Weir EK: Cellular and molecular basis of pulmonary arterial hypertension. J Am Coll Cardiol 2009, 54:S20–S31
28. Thibault HB, Kurtz B, Raher MJ, Shaik RS, Waxman A, Derumeaux G, Halpern EF, Bloch KD, Scherrer-Crosbie M: Noninvasive assessment of murine pulmonary arterial pressure: validation and application to models of pulmonary hypertension. Circ Cardiovasc Imaging 2010, 3: 157–163
29. Fagan KA, Fouty BW, Tyler RC, Morris KG, Jr., Hepler LK, Sato K, LeCras TD, Abman SH, Weinberger HD, Huang PL, McMurtry IF, Rodman DM: The pulmonary circulation of homozygous or heterozygous eNOS-null mice is hyperresponsive to mild hypoxia. J ClinI Invest 1999, 103:291–299
30. Giaid A, Saleh D: Reduced expression of endothelial nitric oxide synthase in the lungs of patients with pulmonary hypertension. N Engl J Med 1995, 333:214–221
31. Shao D, Park JE, Wort SJ: The role of endothelin-1 in the pathogenesis of pulmonary arterial hypertension. Pharmacol Res 2011, 63:504–511
32. Allen SW, Chatfield BA, Koppenhafer SA, Schaffer MS, Wolfe RR, Abman SH: Circulating immunoreactive endothelin-1 in children with pulmonary hypertension. Association with acute hypoxic pulmonary vasoreactivity. Am Rev Respir Dis 1993, 148:519–522
33. Giaid A, Yanagisawa M, Langleben D, Michel RP, Levy R, Shennib H, Kimura S, Masaki T, Duguid WP, Stewart DJ: Expression of endothelin-1 in the lungs of patients with pulmonary hypertension. N Engl J Med 1993, 328:1732–1739
34. Calabro P, Limongelli G, Maddaloni V, Vizza CD, D'Alto M, D'Alessandro R, Poscia R, Argiento P, Ziello B, Badagliacca R, Romeo E, Pacileo G, Russo MG, Fedele F, Calabro R: Analysis of endothelin-1 and endothelin-1 receptor A gene polymorphisms in patients with pulmonary arterial hypertension. Intern Emerg Med 2012, 7:425–430
35. Crosswhite P, Sun Z: Nitric oxide, oxidative stress and inflammation in pulmonary arterial hypertension. J Hypertens 2010, 28:201–212
36. Hassoun PM, Mouthon L, Barbera JA, Eddahibi S, Flores SC, Grimminger F, Jones PL, Maitland ML, Michelakis ED, Morrell NW, Newman JH, Rabinovitch M, Schermuly R, Stenmark KR, Voelkel NF, Yuan JX, Humbert M: Inflammation, growth factors, and pulmonary vascular remodeling. J Am Coll Cardiol 2009, 54:S10–S19
37. Humbert M, Morrell NW, Archer SL, Stenmark KR, MacLean MR, Lang IM, Christman BW, Weir EK, Eickelberg O, Voelkel NF, Rabinovitch M: Cellular and molecular pathobiology of pulmonary arterial hypertension. J Am Coll Cardiol 2004, 43:13S–24S
38. Zhang J, Patel JM: Role of the CX3CL1-CX3CR1 axis in chronic inflammatory lung diseases. Int J Clin Exp Med 2010, 3:233–244
39. Balabanian K, Foussat A, Dorfmuller P, Durand-Gasselin I, Capel F, Bouchet-Delbos L, Portier A, Marfaing-Koka A, Krzysiek R, Rimaniol AC, Simonneau G, Emilie D, Humbert M: CX(3)C

chemokine fractalkine in pulmonary arterial hypertension. Am J Respir Crit Care Med 2002, 165:1419–1425
40. Chandrasekar B, Mummidi S, Perla RP, Bysani S, Dulin NO, Liu F, Melby PC: Fractalkine (CX3CL1) stimulated by nuclear factor kappaB (NF-kappaB)-dependent inflammatory signals induces aortic smooth muscle cell proliferation through an autocrine pathway. Biochem J 2003, 373:547–558
41. Ryu J, Lee CW, Hong KH, Shin JA, Lim SH, Park CS, Shim J, Nam KB, Choi KJ, Kim YH, Han KH: Activation of fractalkine/CX3CR1 by vascular endothelial cells induces angiogenesis through VEGF-A/KDR and reverses hindlimb ischaemia. Cardiovasc Res 2008, 78:333–340
42. Yamashita K, Imaizumi T, Hatakeyama M, Tamo W, Kimura D, Kumagai M, Yoshida H, Satoh K: Effect of hypoxia on the expression of fractalkine in human endothelial cells. Tohoku J Exp Med 2003, 200:187–194
43. Radmark OP: The molecular biology and regulation of 5-lipoxygenase. Am J Respir Crit Care Med 2000, 161:S11–S15
44. Voelkel NF, Tuder RM, Wade K, Hoper M, Lepley RA, Goulet JL, Koller BH, Fitzpatrick F: Inhibition of 5-lipoxygenase-activating protein (FLAP) reduces pulmonary vascular reactivity and pulmonary hypertension in hypoxic rats. J Clin Invest 1996, 97:2491–2498
45. Wright L, Tuder RM, Wang J, Cool CD, Lepley RA, Voelkel NF: 5-Lipoxygenase and 5-lipoxygenase activating protein (FLAP) immunoreactivity in lungs from patients with primary pulmonary hypertension. Am J Respir Crit Care Med 1998, 157:219–229
46. Price LC, Wort SJ, Perros F, Dorfmuller P, Huertas A, Montani D, Cohen-Kaminsky S, Humbert M: Inflammation in pulmonary arterial hypertension. Chest 2012, 141:210–221
47. Koenig M, Joyal F, Fritzler MJ, Roussin A, Abrahamowicz M, Boire G, Goulet JR, Rich E, Grodzicky T, Raymond Y, Senecal JL: Autoantibodies and microvascular damage are independent predictive factors for the progression of Raynaud's phenomenon to systemic sclerosis: a twenty-year prospective study of 586 patients, with validation of proposed criteria for early systemic sclerosis. Arthritis Rheum 2008, 58:3902–3912